

SUPPLEMENTAL MATERIAL

Supplemental Methods

Patients

Hearts were obtained from organ donors whose hearts were explanted to obtain pulmonary and aortic valves for transplant surgery. Before cardiac explantation, organ donors did not receive medication apart from dobutamine, furosemide, and plasma expanders. The investigations conform to the principles of the Declaration of Helsinki. Experimental protocols were approved by the University of Szeged and National Scientific and Research Ethical Review Boards (No. 51-57/1997 OEj and 4991-0/2010-1018EKU (339/PI/010.)). After explantation, each heart was perfused with cardioplegic solution and kept cold (4-6°C) for 2-4 hours prior to dissection. The cardioplegic solution contained (mmol/L): NaCl 110, KCl 16, MgCl₂ 16, CaCl₂ 1.2, NaHCO₃ 10.

Animals

All experiments complied with the *Guide for the Care and Use of Laboratory Animals* (NIH publication No 85-23, revised 1985). The protocols were approved by the review board of the Department of Animal Health and Food Control of the Ministry of Agriculture and Rural Development, Hungary (XII./01031/000/2008 and XIII./1211/2012). Adult mongrel dogs of either sex weighing 8 to 16 kg were anesthetized with pentobarbital (30 mg/kg *i.v.*). Hearts were removed through right lateral thoracotomies and rinsed in oxygenated modified Locke's solution containing (mol/L): Na⁺ 140, K⁺ 4, Ca²⁺ 1.0, Mg²⁺ 1.0, Cl⁻ 126, HCO₃⁻ 25 and glucose 11; pH 7.35-7.45, 95% O₂-5% CO₂, 37°C.

Action Potential Measurements

Action potentials (APs) were recorded in right-ventricular trabeculae and papillary-muscle preparations (<2-mm diameter), from 15 non-diseased human donor hearts (9 male and 6 female, age=44.6±5.9 years) and 25 adult mongrel dogs, with conventional microelectrode techniques.

Trabeculae and papillary muscles were excised and mounted in a tissue chamber (volume ≈ 50 ml) perfused with oxygenated (95% O₂ + 5% CO₂) modified Tyrode's solution containing (in mmol/L): NaCl, 115; KCl, 4; CaCl₂, 1.8; MgCl₂, 1.0; NaHCO₃, 20; and glucose, 11. The pH of this solution was 7.35 to 7.45 at 37°C. Initially, each preparation was stimulated at a basic cycle length of 1000 ms (frequency = 1 Hz), using 2 ms long rectangular constant-voltage pulses isolated from ground and delivered via bipolar platinum electrodes in contact with the preparation using an EMG 4767 type stimulator (Medicor Ltd, Budapest, Hungary). One hour or more was allowed for each preparation to equilibrate while continuously superfused with Tyrode's solution warmed to 37°C. Transmembrane potentials were recorded using conventional 5-20 Mohm, 3 mol/L-KCl filled microelectrodes connected to the input of a high-impedance amplifier (Experimetria Ltd, Budapest, Hungary).

After baseline measurements had been obtained, each preparation was superfused with Tyrode's solution containing a single test drug diluted to the proper concentration for 40 to 60 minutes before measurements were repeated at 3 min intervals in the continued presence of the test drug, until less than a 5% change occurred in action potential characteristics between subsequent samples. When microelectrode impalement was lost, reimpalement was attempted. If action potential characteristics recorded with the new impalement deviating by more than 5% from the preceding ones, the experiment was terminated and results were excluded from evaluation.

Transmembrane-current Measurements

Cell Isolation

Ventricular myocytes were enzymatically dissociated from the left-ventricular midmyocardial free wall of 10 additional non-diseased human donor hearts (5 male and 5 female, age=43.4±5.3 years) and 21 dog hearts.

Canine cardiomyocytes

Ventricular cardiomyocytes were enzymatically dissociated from hearts of mongrel dogs of either sex weighing 8-20 kg following anaesthesia (sodium pentobarbital, 30 mg/kg *i.v.*). The hearts were immediately placed in cold (4°C) solution with the following composition (mmol/L): NaCl 135, KCl 4.0, KH₂PO₄ 1.2, MgSO₄ 1.2, HEPES 10, NaHCO₃ 4.4, Glucose 10, CaCl₂ 1.8, (pH 7.2). A portion of the left-ventricular wall containing an arterial branch large enough to cannulate was then perfused in a modified Langendorff apparatus at a pressure of 60 cm H₂O with solutions in the following sequence: 1) Ca²⁺-containing solution (10 min), 2) Ca²⁺-free solution (10 min), and 3) Ca²⁺-free solution containing collagenase (type I, 0.66 mg/ml, Sigma Chemicals, St. Louis MO) and bovine serum albumin (fraction V, fatty-acid free, 2 mg/ml, Sigma) (15 min). Protease (type XIV, 0.12 mg/ml, Sigma) was added to the final perfusate and another 15-30 min of digestion was allowed. Portions of the left-ventricular wall judged to be well-digested were diced into small pieces and placed either in Kraft-Brühe (KB) solution or in Ca²⁺-free solution supplemented with CaCl₂ (1.25 mmol/L) for 15 minutes. Next, these tissue samples were gently agitated in a small beaker to dislodge single myocytes from the extracellular matrix. During the entire isolation procedure, solutions were gassed with 100% O₂, while their temperatures were maintained at 37°C. Myocytes were allowed to settle to the bottom of the beaker for 10 minutes, and then half of the supernatant was replaced with fresh

solution. This procedure was repeated three times. Myocytes placed in KB solution were stored at 4°C; those placed in Tyrode's solution were maintained at 12-14°C prior to experimentation. Cells that were stored in KB solution or immediately placed in 1.25-mol/L Ca²⁺-containing solution had the same appearance and there were no discernible differences in their characteristics.

The composition of the solutions used for cell isolation was (in mmol/L):

- a) Ca²⁺ containing solution - NaCl 135, KCl 4.7, KH₂PO₄ 1.2, MgSO₄ 1.2, HEPES 10, NaHCO₃ 4.4, glucose 10, taurine 20 and CaCl₂ 1.0 (pH 7.2 adjusted with NaOH);
- b) Ca²⁺-free solution - NaCl 135, KCl 4.7, KH₂PO₄ 1.2, MgSO₄ 1.2, HEPES 10, NaHCO₃ 4.4, Glucose 10, and taurine 20 (pH 7.2 adjusted with NaOH);
- c) KB solution - KOH 90, L-glutamic acid 70, taurine 15, KCl 30, KH₂PO₄ 10, MgCl₂ 0.5, HEPES 10, glucose 11, and EGTA 0.5 (pH 7.3 adjusted with KOH);

Human cardiomyocytes

After explantation and removal of the valves, hearts were transported into the laboratory in cold (4°C) cardioplegic solution. The isolation procedure was in general similar to that used in obtaining dog ventricular myocytes. The only difference was that the enzyme containing solution was supplemented with elastase (type III, 0.045 mg/ml, Sigma) and the second step of digestion was usual longer (45-90 min) than used in obtaining dog cardiac cells.

Experimental Procedures

Myocytes were placed in a recording chamber on the stage of inverted microscopes (Nikon-TMS or Olympus IX51) and allowed to adhere. Only rod-shaped, clearly striated myocytes (average

length = 100 μm , diameter = 20 μm) were used for recording. Although the yield varied greatly (from 5 to 70%) between each dissociation procedure, the ease of electrode-seal formation and the quality of the measurements obtained did not correlate with yield. Micropipettes were fabricated from borosilicate glass capillaries (Clark Electromedical Instruments, Pangbourne, Reading, UK) using a microprocessor controlled horizontal puller (Sutter Instruments, Novato, CA). The electrodes had resistances between 1.5 and 2.5 MOhm when filled with the pipette solution. Membrane currents were recorded with Axopatch-1D and Axopatch 200B patch-clamp amplifiers (Axon Instruments, Union City, CA) in the whole-cell patch-clamp configuration. After establishing a high (1-10 GOhm) resistance seal by gentle suction, the cell membrane beneath the tip of the electrode was disrupted by additional suction or application of 1.5 V electrical pulses for 1-5 ms. Series resistance was typically 4 to 8 MOhm before compensation (usually 50-80%). When the initial series resistance was greater than 10 MOhm, or when series resistance increased substantially during measurement, the experiment was terminated, and the results were excluded from analyses. Membrane currents were digitized using a 333 kHz analogue-to-digital converter (Digidata 1200 or 1322A, Axon Instruments) with commercial software (pClamp 6.0 and 8.0, Axon Instruments), and results were analyzed using the same software after low-pass (1 kHz) filtering.

Solutions for measuring K^+ -currents

HEPES-buffered Tyrode's solution (in mmol/L: NaCl 144, NaH_2PO_4 0.33, KCl 4.0, CaCl_2 1.8, MgCl_2 0.53, Glucose 5.5, and HEPES 5.0 at pH 7.4.) served as external solution and normal K-aspartate containing (in mmol/L K-aspartate 100, KCl 20, MgATP 5, EGTA 5, HEPES 10, and glucose 5, pH adjusted to 7.2 with KOH) as internal pipette solution. Superfusion was maintained by gravity flow at approximately 2-2.5 ml/min. The external solution contained 1 $\mu\text{mol/L}$ nisoldipine (Bayer AG,

Germany) to completely block L-type Ca^{2+} -current (I_{CaL}). I_{Kr} and I_{Ks} were separated pharmacologically by adding 100 nmol/L L-735,821 or 500 nmol/L HMR-1556 (selective I_{Ks} -blockers) or 1 $\mu\text{mol/L}$ E-4031 or 100 nmol/L dofetilide (I_{Kr} -blockers) to the external solution. The inward Na^+ current (I_{Na}) was inactivated using a -40 mV holding potential, which also largely inactivated the transient outward current (I_{to}).

Solutions for measuring Ca^{2+} -currents

HEPES-buffered Tyrode solution containing (in mmol/L): NaCl, 140; KCl, 5.4, CaCl_2 , 2.5; MgCl_2 , 1.2; Na_2HPO_4 , 0.35; HEPES, 5; glucose, 10 at pH 7.4, supplemented with 3 mmol/L 4-aminopyridine) served as external solution. The electrodes were filled with an internal solution containing in mmol/L: KCl, 110; KOH, 40; K-ATP, 3; HEPES, 10; EGTA, 10; tetraethylammonium chloride (TEACl), 20; glucose, 5; GTP, 0.25. The pH of the internal solution was adjusted to 7.2 with KOH.

Measuring $\text{Na}^+/\text{Ca}^{2+}$ -exchanger current

To record the $\text{Na}^+/\text{Ca}^{2+}$ -exchanger (NCX) current, the method of Hobai et al (Pflugers Arch. 433, 455-463, 1997) was applied, with K^+ -free bath (in nmol/L: NaCl 135, CsCl 10, CaCl_2 1, MgCl_2 1, BaCl_2 0.2, NaH_2PO_4 0.33, TEACl 10, HEPES 10, glucose 10 and in $\mu\text{mol/L}$: ouabain 20, nisoldipine 1, Lidocaine 50; at pH 7.4;) and pipette solutions (mmol/L: CsOH 140, aspartic acid 75, TEACl 20, MgATP 5, HEPES 10, NaCl 20, EGTA 20, CaCl_2 , 10; pH adjusted to 7.2 with CSOH) were used in order to block the Na-, Ca-, K-currents and the Na/K pump current. The I-V relationship of I_{NCX} was measured by ramp pulses with 20-s intervals. The ramp pulse initially depolarized from the holding potential of -40 mV to 60 mV (1 s in duration), then hyperpolarized to -140 mV (2 s in duration), and then depolarized back to the holding potential. The NCX current was defined as the Ni^{2+} -sensitive

current *i.e.* subtracting values recorded in the presence of 10 mM NiCl₂ from those measured in the absence of NiCl₂. In separate experiments, changes in the Ni²⁺ insensitive current were also assessed.

Molecular Biology

Reverse Transcription (RT)-Quantitative Polymerase Chain-reaction (qPCR)

Left-ventricular midmyocardial free-wall samples were obtained from 12 human (7 male and 5 female, age=45.2±3.7 years) and 8 dog hearts, and snap-frozen in liquid-N₂. RNA was isolated with the Qiagen RNase Tissue kit (Amersham Pharmacia Biotech, Piscataway, NJ). Reverse-transcription (RT) was performed with Superscript-II RNase H-Reverse Transcriptase (Invitrogen). Gene-specific primers were designed with Primer-Express (Applied Biosystems) and synthesized by Bioneer Laboratory (Buckingham, UK) for *KCNJ* and *β-actin* genes, by Applied Biosystems (Warrington, UK) for *KCNH2*, *KCNQ1* and *KCNE1* genes (On-line Table 1).

QPCR was performed on a RotorGene-3000 instrument (Corbett Research, Australia) with gene-specific primers and SybrGreen. Expression-values were normalized to *β-actin* data obtained on the same samples (n=8/amplicon). Triplicate standard curves were run for each experiment. Data analysis was performed with Rotor-Gene Analysis Software V6.0 and Pfaffl method, correcting for amplification-efficiency differences.

Western Blot

Membrane proteins were obtained from the same samples used for qPCR. Samples were suspended in lysis buffer (mmol/L): 20 Tris-Cl, 1 EDTA, 0.008 aprotinin, 20 leupeptin, 1×protease inhibitor cocktail and 5 µg/L Na-vanadate (Sigma Chemical, St. Louis, MO), dounced and centrifuged (2000×g, 10 min, 4°C). The supernatant was resuspended in lysis buffer containing 2%-Triton X-100. After

1.5-hour incubation on ice, samples were ultracentrifuged (100,000×g, 35 min, 4°C), supernatants collected and stored at -70°C. Protein-concentration was measured by Lowry method and samples diluted in loading buffer for SDS-polyacrylamide gel electrophoresis (PAGE) on 8% or 10% acrylamide/bis-acrylamide gels. Fractionated proteins were transferred onto polyvinylidene difluoride (PVDF) membranes (Immobilon-P, Millipore). Blots were blocked in Tris-buffer supplemented with Tween-20 (TBST) and 10% non-fat milk (BioRad, USA), then incubated overnight (4°C) with rabbit polyclonal primary antibody against Kir2.1, Kir2.2, Kir2.3, ERG, minK and KvLQT1 (Alomone Labs, Israel; dilution 1:100), goat anti-Kir2.4 (Santa Cruz Biotechnology) or mouse monoclonal anti- α -sarcomeric actin (DAKO). ERGa- and ERGb-specific bands were identified by blotting membranes with the ERG antibody pre-incubated with the control peptide (Supplemental Figure 7). Bound primary antibodies were detected by incubating with anti-rabbit, anti-goat or anti-mouse secondary antibodies (IgGs) conjugated to horseradish peroxidase (DAKO; 1 hour, room temperature). Immunoreactivity was visualised with enhanced chemoluminescence (ECL-Plus, Amersham-Pharmacia). Analysis was performed with ImageJ™. All values were quantified relative to an internal control on the same sample (α -actin for Kir2.x, KvLQT1 and minK, GAPDH for ERG).

Immunohistochemistry

Isolated dog (n=6) and human (3 male, 1 female, age=48.3±4.7 years) left-ventricular midmyocardial free-wall ventricular cardiomyocytes were settled on glass coverslips and fixed with acetone. Samples were rehydrated with calcium-free phosphate-buffered saline (PBS) and blocked for 2 hours with PBST (PBS with 0.01% Tween) containing 1% BSA (Bovine serum albumin, Sigma) at room temperature. Immunofluorescent-staining was obtained with polyclonal rabbit anti-Kir2.1, anti-Kir2.2, anti-Kir2.3, anti-ERG, anti-KvLQT1 and anti-minK (Alomone), 1:50 dilution, and a fluorescent secondary antibody

(Alexafluor 448-conjugated goat anti-rabbit IgG, 1:1000 dilution, Molecular Probes). Incubation with the primary antibody for 1.5 hours at room temperature was followed by 1-hour incubation with secondary antibodies and thorough washing with PBST. Control samples were incubated only with secondary antibody (Supplemental Figure 2).

Fluorescent images were obtained with an Olympus FV1000 confocal laser-scanning microscope and standardized parameter settings. Images were quantified in greyscale TIFF format (Adobe Photoshop) with ImageQuantTM-software (Molecular Dynamics). On each image, three to five random strips were selected and fluorescent profiles plotted. On the profile-plots the baseline pixels were identified and subtracted from total profile area.

Mathematical modelling

To assess the contribution of ionic-current components to repolarization-reserve in human versus canine hearts two different largely used mathematical modeling approaches have been attempted.

1. The Hund-Rudy model

The control dog ionic model is based on the Hund-Rudy dynamic (HRd) canine ventricular model (Hund and Rudy, 2004). The Matlab implementation was downloaded from Y. Rudy's website (<http://rudylab.wustl.edu/>) and numerically integrated using the ODE15s scheme for stiff systems with absolute and relative tolerance of 10^{-4} . A human-like formulation was derived based on our new data. Factors (α) scale the maximum conductance of the labelled currents and are summarized in Table 1. Ito level in the HRd model was based on epicardic measurements (Lue and Boyden, 1992). In this study,

I_{to} was scaled down to 0.9 of the published HRd canine model to reproduce the level found at the canine subendocardium (Xiao et al, 2008).

Table 1. Scaling values for currents modified in the HRd ionic model.

	$\alpha_{ICa,L}$	α_{Ito}	α_{IKs}	α_{IK1}
Dog	1.0	0.900	1.0	1.0
Human	1.3	0.693	0.22	0.3779

Ionic current block by drugs was introduced in the ionic modeling by scaling the maximum currents with the following factors: 0.5 (I_{Kr} -block), 0.3 (I_{K1} -block), 0.5 (I_{Ks} -block).

2. The O'Hara-Rudy model

The control human ionic model is based on the O'Hara-Rudy dynamic (ORd) human ventricular model (O'Hara et al, 2011). The Matlab implementation was downloaded from Y. Rudy's website (<http://rudylab.wustl.edu/>) and numerically integrated using the ODE15s scheme for stiff systems with absolute and relative tolerance of 10^{-4} . A canine-like formulation was derived based on our new data. Factors (α) scale the maximum conductance of the labelled currents and are summarized in Table 2.

Table 2. Scaling values for currents modified in the ORd ionic model.

	$\alpha_{ICa,L}$	α_{Ito}	α_{IKs}	α_{IK1}
Dog	0.7692	1.3	4.5455	2.6462
Human	1.0	1.0	1.0	1.0

Ionic current block by drugs was introduced in the ionic modelling by scaling the maximum currents with the following factors: 0.5 (I_{Kr} -block), 0.3 (I_{K1} -block), 0.5 (I_{Ks} -block).

Statistics

Results are expressed as mean \pm SEM. Statistical significance was determined by two-tailed Student's *t*-tests and ANOVA where appropriate. Results were considered significant for $P < 0.05$.

References

- Hund TJ, Rudy Y (2004). Rate dependence and regulation of action potential and calcium transient in a canine cardiac ventricular cell model. *Circulation* **110**, 3168-3174.
- Lue WM, Boyden PA. Abnormal electrical properties of myocytes from chronically infarcted canine heart. Alterations in V_{max} and the transient outward current. *Circulation* **85**, 1175-1188.
- O'Hara T, Virág L, Varró A, Rudy Y (2011). Simulation of the undiseased human cardiac ventricular action potential: model formulation and experimental validation. *PLoS Comput Biol* **7(5)** e1002061.
- Xiao L, Coutu P, Villeneuve LR, Tadevosyan A, Maguy A, Le Bouter S, Allen BG, Nattel S (1998). Mechanisms underlying rate-dependent remodeling of transient outward potassium current in canine ventricular myocytes. *Circ Res* **103**, 733-742.

Supplemental Figure Legends

Supplemental Figure 1: Concentration-response curve for APD-prolongation by dofetilide in human and canine ventricular cardiomyocytes.

Supplemental Figure 2: Negative controls for immunostaining measurements performed by immunofluorescence confocal-microscope. Negative control samples (only the secondary fluorescent labeled antibody were applied) for Figure 6. Corresponding Dark-field images of typical human and dog ventricular cardiomyocytes are shown at the bottom.

Supplemental Figure 3. Kinetics of recovery from inactivation of I_{to} and I_{Ca} currents in human and dog ventricular myocytes. Panel A. Original recordings of I_{to} recovery kinetics in human (top) and dog (bottom) myocytes . Insets show the applied voltage protocols. Corresponding mean \pm SEM time constant values are given also as inset calculated on the average of 9-16 human and dog cells. Panel B. Original recordings of I_{Ca} recovery kinetics in human (top) and dog (bottom) myocytes. Insets show the applied voltage protocols. Corresponding mean \pm SEM time constant values are given also as inset calculated on the average of 1 and 6 human and dog cells, respectively.

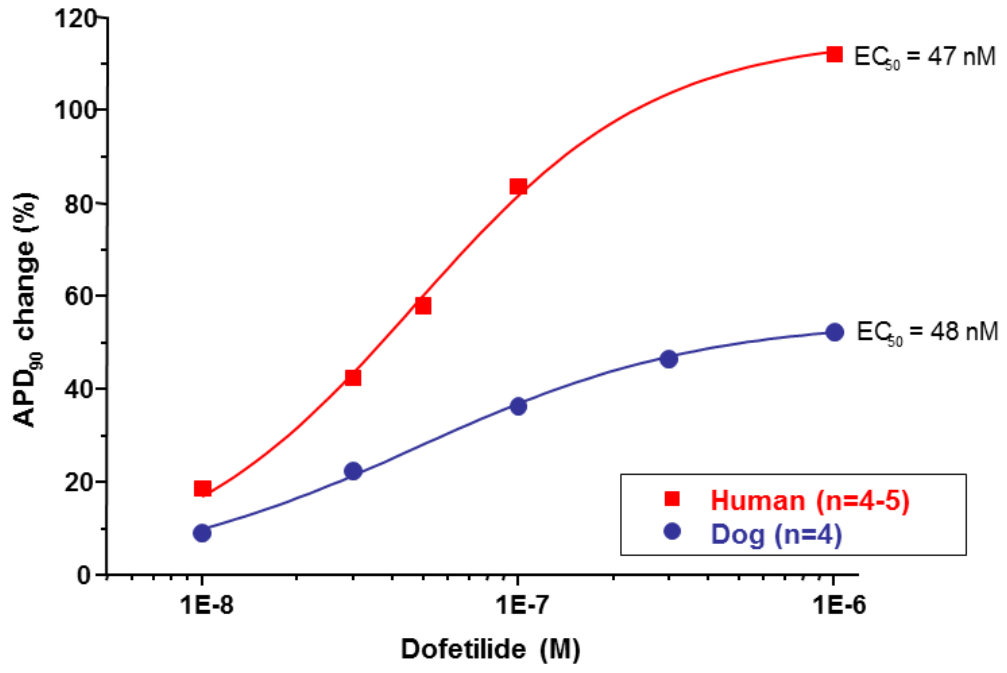
Supplemental Figure 4: Simulations of effect of combined $I_{Kr} + I_{K1}$ and $I_{Kr} + I_{Ks}$ inhibition on human and dog ventricular-muscle APs by applying the Hund-Rudy dynamic (HRd) canine ventricular-AP model. **Panel A.** Simulated human APs at control, following I_{K1} -block (70%-reduction), I_{Kr} -block (50 %-reduction), and combined I_{K1}/I_{Kr} -block. **Panel B.** Corresponding data for dog I_{K1}/I_{Kr} -block.

Panel C. Simulated human APs at control, following I_{Ks} -block (50%-reduction), I_{Kr} -block (50%-reduction), and combined I_{Ks}/I_{Kr} -block. **Panel D.** Corresponding data for dog I_{Ks}/I_{Kr} -block.

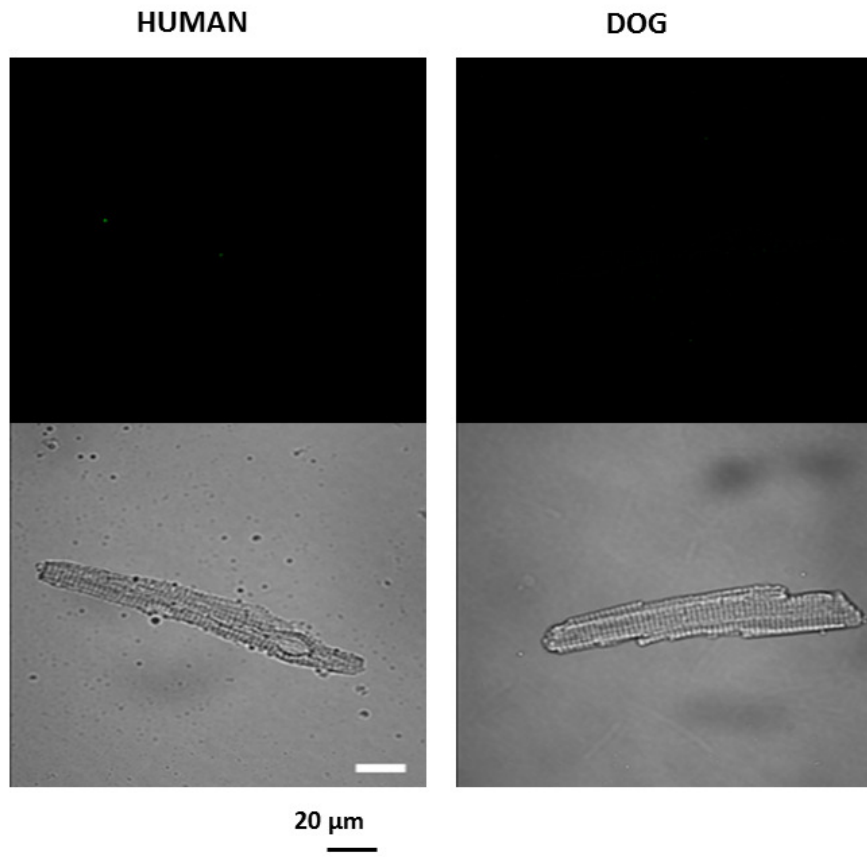
Supplemental Figure 5: Simulation of the role of I_{CaL} and I_{to} in the effects of I_{Kr} inhibition on human and dog ventricular-muscle APs at 1Hz by applying the Hund-Rudy dynamic (HRd) canine ventricular-AP model. **Panel A.** Simulated dog APs at control and following I_{Kr} -block (50% reduction). **Panel B.** Corresponding data for human AP. The human AP-model was obtained by adjusting I_{Ks} I_{K1} I_{to} and I_{CaL} in the canine model according to the current-density differences obtained with direct recordings. **Panel C.** Simulated human APs with I_{CaL} set back to canine values, at control and following I_{Kr} -block (50%-reduction). **Panel D.** Simulated human APs with I_{to} set back to canine values, at control and following I_{Kr} -block (50%-reduction).

Supplemental Figure 6: Simulation of the role of I_{CaL} and I_{to} in the effects of I_{Kr} inhibition on human and dog ventricular-muscle APs at 1Hz by applying the O'Hara-Rudy dynamic (ORd) human ventricular-AP model. **Panel A.** Simulated dog APs at control and following I_{Kr} -block (50% reduction). **Panel B.** Corresponding data for human AP. The human AP-model was obtained by adjusting I_{Ks} I_{K1} I_{to} and I_{CaL} in the canine model according to the current-density differences obtained with direct recordings. **Panel C.** Simulated human APs with I_{CaL} set back to canine values, at control and following I_{Kr} -block (50%-reduction). **Panel D.** Simulated human APs with I_{to} set back to canine values, at control and following I_{Kr} -block (50%-reduction).

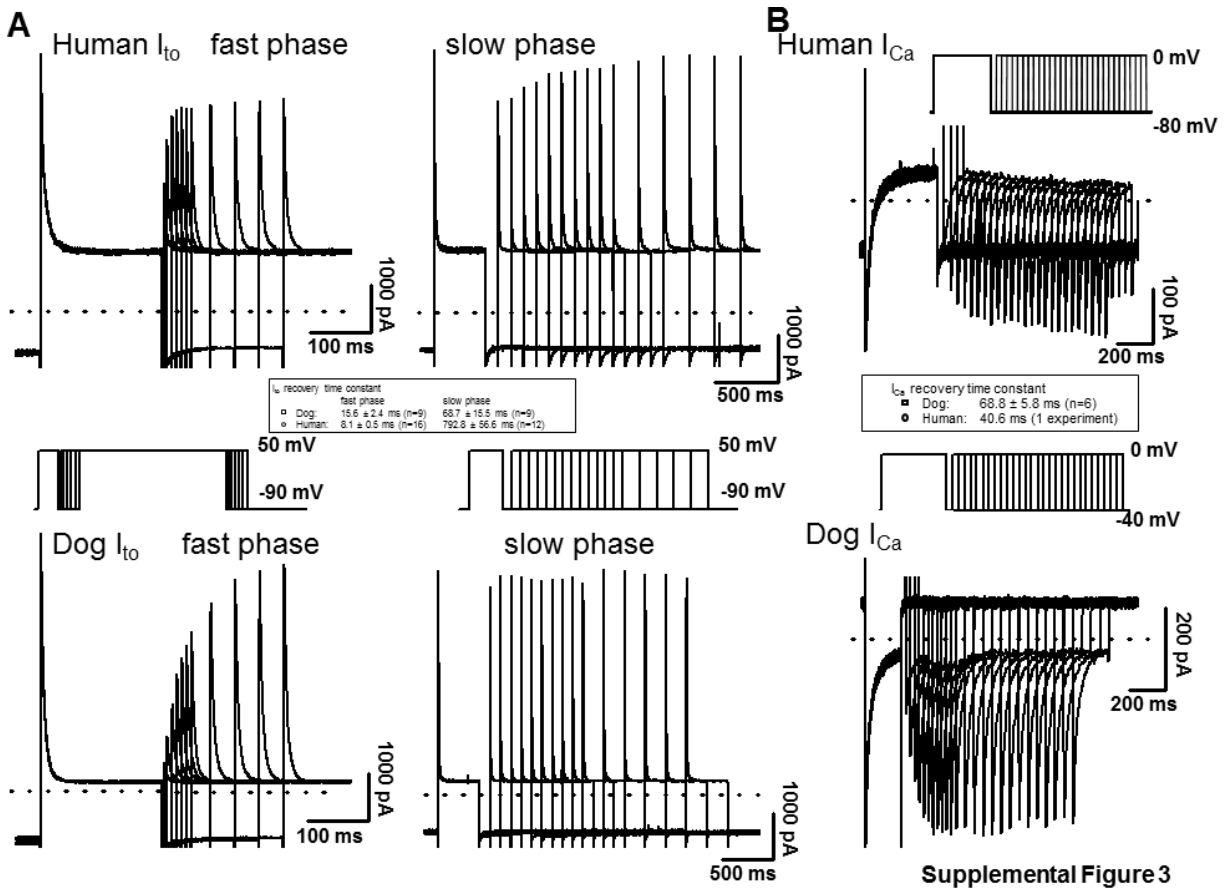
Supplemental Figure 7: Identification of bands corresponding to ERGa and ERGb isoforms in dog and human samples. Equal amounts of human and canine protein samples were loaded on the gel and were blotted to PVDF membrane. Before the immunolabeling procedure, the membrane was cut and was probed with 1 ug of hERG antibody with and without pre-incubation with the control peptide (0, 3 or 6 μ g) H: human; C: canine samples.



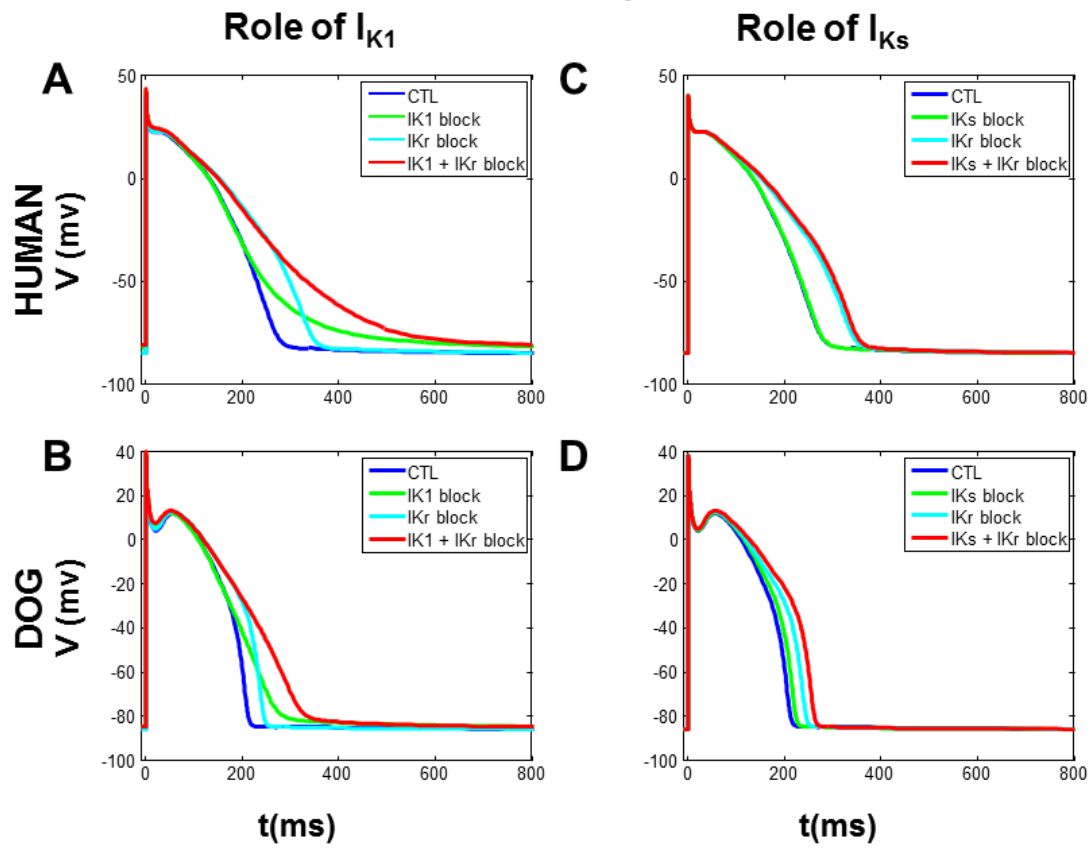
Supplemental Figure 1



Supplemental Figure 2

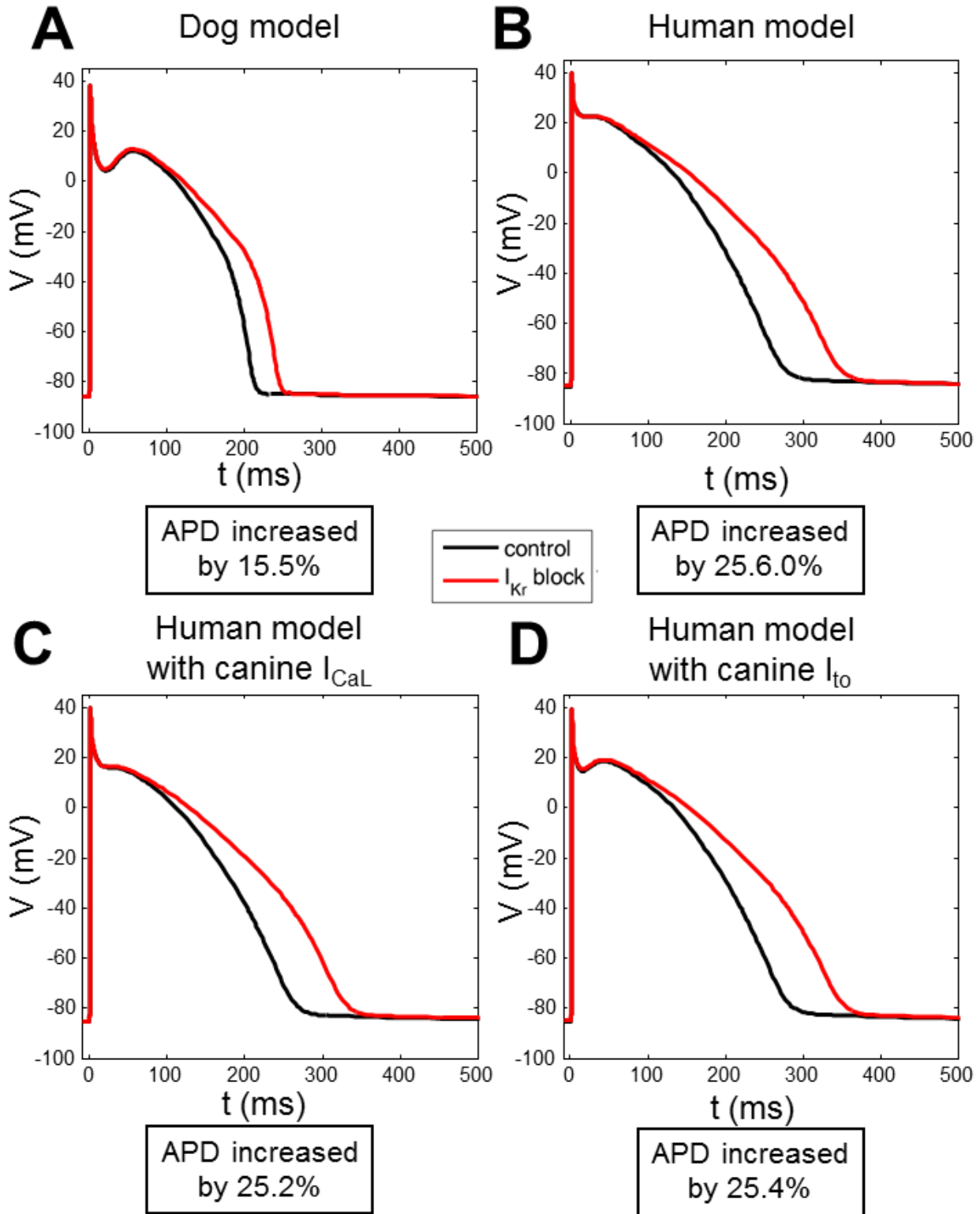


Hund-Rudy model



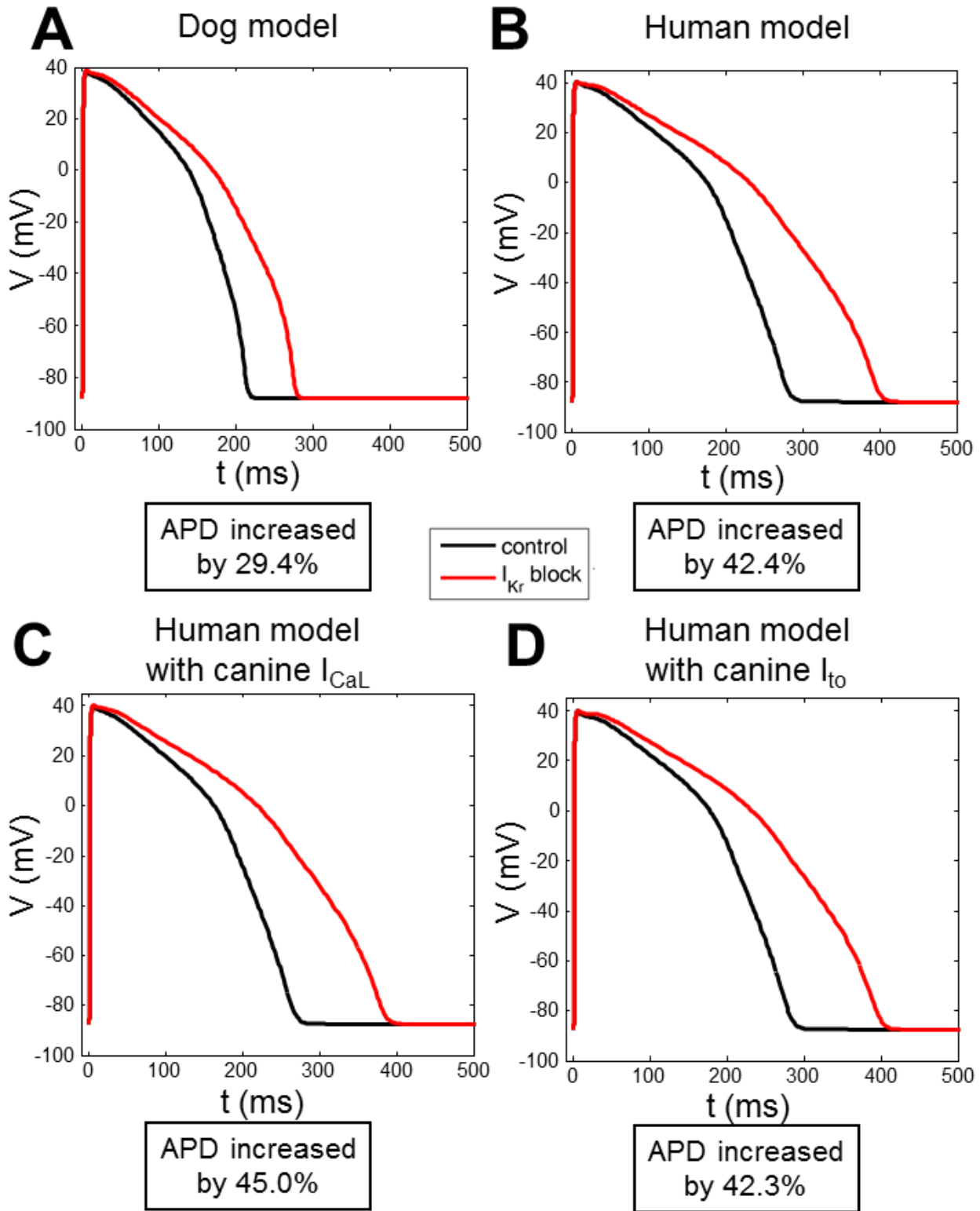
Supplemental Figure 4

Hund-Rudy model

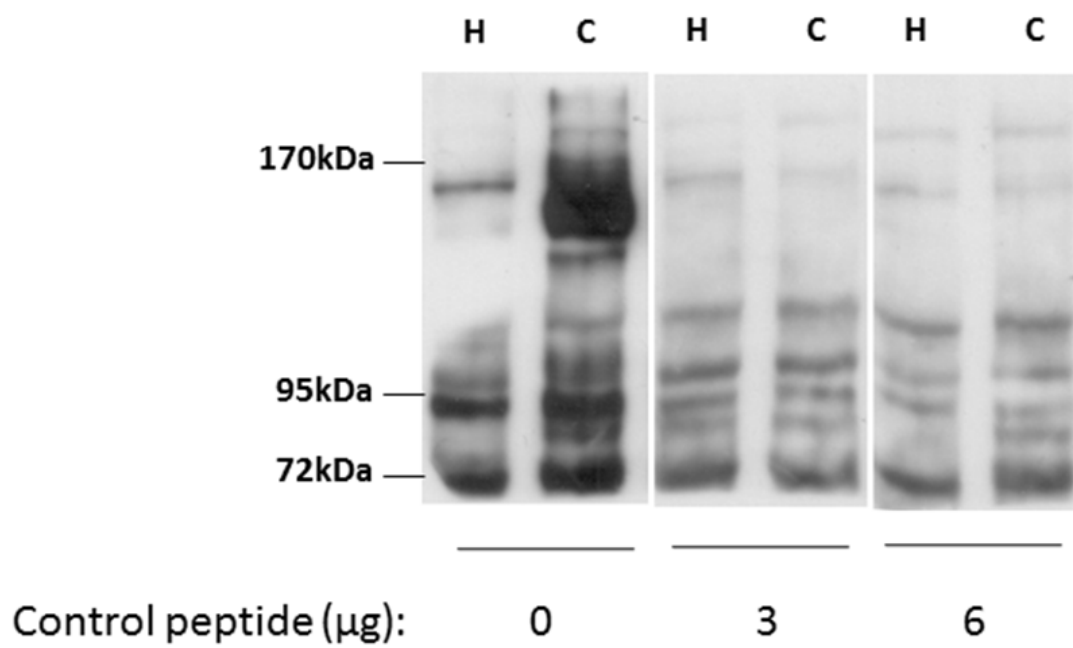


Supplemental Figure 5

O'Hara model



Supplemental Figure 6

**Supplemental Figure 7**